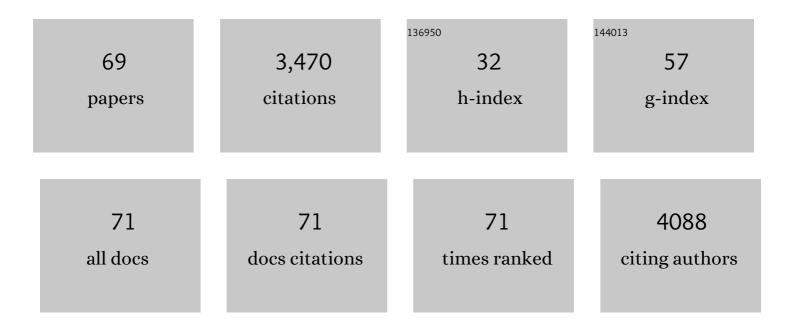
## List of Publications by Year in descending order

Source: https://exaly.com/author-pdf/8117030/publications.pdf Version: 2024-02-01



#	Article	IF	CITATIONS
1	Denatured proteins show new vitality: Green synthesis of germanium oxide hollow microspheres with versatile functions by denaturing proteins around bubbles. Aggregate, 2023, 4, .	9.9	8
2	ZIF-8@GMP-Tb nanocomplex for ratiometric fluorescent detection of alkaline phosphatase activity. Spectrochimica Acta - Part A: Molecular and Biomolecular Spectroscopy, 2022, 264, 120230.	3.9	15
3	Taking full advantage of the structure and multi-activities of mineralized microbial surface-displayed enzymes: Portable three-in-one organophosphate pesticides assay device. Chemical Engineering Journal, 2022, 429, 132317.	12.7	12
4	Graphene-Based Nanomaterials for Dental Applications: Principles, Current Advances, and Future Outlook. Frontiers in Bioengineering and Biotechnology, 2022, 10, 804201.	4.1	15
5	Selective Inhibition toward Dual Enzyme-like Activities of Iridium Nanozymes for a Specific Colorimetric Assay of Malathion without Enzymes. Journal of Agricultural and Food Chemistry, 2022, 70, 3898-3906.	5.2	26
6	Flow-homogeneous electrochemical sensing system based on 2D metal-organic framework nanozyme for successive microRNA assay. Biosensors and Bioelectronics, 2022, 206, 114120.	10.1	26
7	A low-background fluorescent aptasensor for acetamiprid detection based on DNA three-way junction-formed G-quadruplexes and graphene oxide. Analytical and Bioanalytical Chemistry, 2021, 413, 2071-2079.	3.7	14
8	Catalyst-Free Spontaneous Polymerization with 100% Atom Economy: Facile Synthesis of Photoresponsive Polysulfonates with Multifunctionalities. Jacs Au, 2021, 1, 344-353.	7.9	14
9	Crystal Violet-Sensitized Direct Z-Scheme Heterojunction Coupled with a G-Wire Superstructure for Photoelectrochemical Sensing of Uracil-DNA Glycosylase. ACS Applied Materials & Interfaces, 2021, 13, 15881-15889.	8.0	18
10	Displaying of acetylcholinesterase mutants on surface of yeast for ultra-trace fluorescence detection of organophosphate pesticides with gold nanoclusters. Biosensors and Bioelectronics, 2020, 148, 111825.	10.1	60
11	pH-induced aggregation of hydrophilic carbon dots for fluorescence detection of acidic amino acid and intracellular pH imaging. Materials Science and Engineering C, 2020, 108, 110401.	7.3	28
12	Smartphones and Test Paper-Assisted Ratiometric Fluorescent Sensors for Semi-Quantitative and Visual Assay of Tetracycline Based on the Target-Induced Synergistic Effect of Antenna Effect and Inner Filter Effect. ACS Applied Materials & Interfaces, 2020, 12, 47099-47107.	8.0	105
13	A ratiometric optical strategy for bromide and iodide ion sensing based on target-induced competitive coordination of a metal–organic nanosystem. Journal of Materials Chemistry C, 2020, 8, 11517-11524.	5.5	9
14	Redox induced dual-signal optical sensor of carbon dots/MnO2 nanosheets based on fluorescence and second-order scattering for the detection of ascorbic acid. Mikrochimica Acta, 2020, 187, 475.	5.0	11
15	Multifunctional Binding Strategy on Nonconjugated Polymer Nanoparticles for Ratiometric Detection and Effective Removal of Mercury Ions. Environmental Science & Technology, 2020, 54, 10270-10278.	10.0	45
16	Catalase active metal-organic framework synthesized by ligand regulation for the dual detection of glucose and cysteine. Analytica Chimica Acta, 2020, 1131, 118-125.	5.4	12
17	A label-free photoelectrochemical immunosensor for detection of the milk allergen β-lactoglobulin based on Ag2S -sensitized spindle-shaped BiVO4/BiOBr heterojunction by an in situ growth method. Analytica Chimica Acta, 2020, 1140, 122-131.	5.4	22
18	A lanthanide coordination polymer as a ratiometric fluorescent probe for rapid and visual sensing of phosphate based on the target-triggered competitive effect. Journal of Materials Chemistry C, 2020, 8, 13063-13071.	5.5	39

#	Article	IF	CITATIONS
19	White Peroxidaseâ€Mimicking Nanozymes: Colorimetric Pesticide Assay without Interferences of O <sub>2</sub> and Color. Advanced Functional Materials, 2020, 30, 2001933.	14.9	105
20	A visual detection of human immunodeficiency virus gene using ratiometric method enabled by phenol red and target-induced catalytic hairpin assembly. Talanta, 2020, 219, 121202.	5.5	12
21	White Peroxidaseâ€Mimicking Nanozymes: White Peroxidaseâ€Mimicking Nanozymes: Colorimetric Pesticide Assay without Interferences of O <sub>2</sub> and Color (Adv. Funct. Mater. 28/2020). Advanced Functional Materials, 2020, 30, 2070184.	14.9	5
22	Colorimetric Assay of Bacterial Pathogens Based on Co <sub>3</sub> O <sub>4</sub> Magnetic Nanozymes Conjugated with Specific Fusion Phage Proteins and Magnetophoretic Chromatography. ACS Applied Materials & Interfaces, 2020, 12, 9090-9097.	8.0	95
23	Three–dimensional donor–acceptor–type photoactive material/conducting polyaniline hydrogel complex for sensitive photocathodic enzymatic bioanalysis. Biosensors and Bioelectronics, 2020, 158, 112179.	10.1	21
24	Fe(III) Mixed IP6@Au NPs with Enhanced SERS Activity for Detection of 4-ATP. Scientific Reports, 2020, 10, 5752.	3.3	17
25	Specific phages-based electrochemical impedimetric immunosensors for label-free and ultrasensitive detection of dual prostate-specific antigens. Sensors and Actuators B: Chemical, 2019, 297, 126727.	7.8	35
26	Simultaneous detection of five flavoring agents in chewing gum by ultrasound-microwave synergistic extraction coupled with gas chromatography. Scientific Reports, 2019, 9, 12085.	3.3	4
27	A universal one-pot assay strategy based on bio-inorganic cascade catalysts for different analytes by changing pH-dependent activity of enzymes on enzyme mimics. Sensors and Actuators B: Chemical, 2019, 286, 460-467.	7.8	22
28	Carbon dots-based fluorescent turn off/on sensor for highly selective and sensitive detection of Hg2+ and biothiols. Spectrochimica Acta - Part A: Molecular and Biomolecular Spectroscopy, 2019, 222, 117260.	3.9	33
29	Construction of an effective ratiometric fluorescent sensing platform for specific and visual detection of mercury ions based on target-triggered the inhibition on inner filter effect. Journal of Hazardous Materials, 2019, 376, 170-177.	12.4	47
30	pH-mediated reversible fluorescence nanoswitch based on inner filter effect induced fluorescence quenching for selective and visual detection of 4-nitrophenol. Journal of Hazardous Materials, 2019, 362, 45-52.	12.4	130
31	Oxidation etching induced dual-signal response of carbon dots/silver nanoparticles system for ratiometric optical sensing of H2O2 and H2O2-related bioanalysis. Analytica Chimica Acta, 2019, 1055, 81-89.	5.4	29
32	pH-sensitive fluorescent organic nanoparticles: Off-on fluorescent detection of furfural in transformer oil. Talanta, 2019, 197, 383-389.	5.5	8
33	Green fluorescent carbon quantum dots as a label-free probe for rapid and sensitive detection of hematin. Spectrochimica Acta - Part A: Molecular and Biomolecular Spectroscopy, 2019, 212, 167-172.	3.9	20
34	A hybrid materialÂcomposed of guanine-rich single stranded DNA and cobalt(III) oxyhydroxide (CoOOH) nanosheets as a fluorescentÂprobe for ascorbic acid via formation of a complex between G-quadruplex and thioflavin T. Mikrochimica Acta, 2019, 186, 156.	5.0	10
35	Size-dependent modulation of fluorescence and light scattering: a new strategy for development of ratiometric sensing. Materials Horizons, 2018, 5, 454-460.	12.2	69
36	Proteinâ€Directed Metal Oxide Nanoflakes with Tandem Enzymeâ€Like Characteristics: Colorimetric Glucose Sensing Based on Oneâ€Pot Enzymeâ€Free Cascade Catalysis. Advanced Functional Materials, 2018, 28, 1800018.	14.9	227

#	Article	IF	CITATIONS
37	A novel electrochemical sensor based on poly(p-aminobenzene sulfonic acid)-reduced graphene oxide composite film for the sensitive and selective detection of levofloxacin in human urine. Journal of Electroanalytical Chemistry, 2018, 817, 141-148.	3.8	44
38	Selected landscape phage probe as selective recognition interface for sensitive total prostate-specific antigen immunosensor. Biosensors and Bioelectronics, 2018, 106, 1-6.	10.1	34
39	Sensitive colorimetric immunoassay of <i>Vibrio parahaemolyticus</i> based on specific nonapeptide probe screening from a phage display library conjugated with MnO <sub>2</sub> nanosheets with peroxidase-like activity. Nanoscale, 2018, 10, 2825-2833.	5.6	60
40	Rational design of engineered microbial cell surface multi-enzyme co-display system for sustainable NADH regeneration from low-cost biomass. Journal of Industrial Microbiology and Biotechnology, 2018, 45, 111-121.	3.0	10
41	Enzymatic biofuel cell-based self-powered biosensing of protein kinase activity and inhibition <i>via</i> thiophosphorylation-mediated interface engineering. Chemical Communications, 2018, 54, 5438-5441.	4.1	23
42	A Thioflavin T-induced G-Quadruplex Fluorescent Biosensor for Target DNA Detection. Analytical Sciences, 2018, 34, 149-153.	1.6	20
43	Redesigning of Microbial Cell Surface and Its Application to Whole-Cell Biocatalysis and Biosensors. Applied Biochemistry and Biotechnology, 2018, 185, 396-418.	2.9	74
44	Preparation of a Si/SiO <sub>2</sub> –Orderedâ€Mesoporousâ€Carbon Nanocomposite as an Anode for Highâ€Performance Lithiumâ€Ion and Sodiumâ€Ion Batteries. Chemistry - A European Journal, 2018, 24, 4841-4848.	3.3	70
45	Mechanistic Insights into Interactions between Bacterial Class I P450 Enzymes and Redox Partners. ACS Catalysis, 2018, 8, 9992-10003.	11.2	78
46	"Nonâ€Naked―Gold with Glucose Oxidase‣ike Activity: A Nanozyme for Tandem Catalysis. Small, 2018, 1 e1803256.	.4, <sub>10.0</sub>	156
47	Rational Integration of Biomineralization, Microbial Surface Display, and Carbon Nanocomposites: Ultrasensitive and Selective Biosensor for Traces of Pesticides. Advanced Materials Interfaces, 2018, 5, 1801332.	3.7	5
48	New approaches to NAD(P)H regeneration in the biosynthesis systems. World Journal of Microbiology and Biotechnology, 2018, 34, 141.	3.6	24
49	Copper nanoclusters with strong fluorescence emission as a sensing platform for sensitive and selective detection of picric acid. Analytical Methods, 2018, 10, 4251-4256.	2.7	36
50	One-step synthesis of fluorescent organic nanoparticles: The application to label-free ratiometric fluorescent pH sensor. Sensors and Actuators B: Chemical, 2018, 273, 1479-1486.	7.8	25
51	Bioinspired Nanozymes with pHâ€Independent and Metal Ionsâ€Controllable Activity: Fieldâ€Programmable Logic Conversion of Sole Logic Gate System. Particle and Particle Systems Characterization, 2018, 35, 1800207.	2.3	16
52	Novel Cell–Inorganic Hybrid Catalytic Interfaces with Enhanced Enzymatic Activity and Stability for Sensitive Biosensing of Paraoxon. ACS Applied Materials & Interfaces, 2017, 9, 6894-6901.	8.0	38
53	Protein-directed gold nanoparticles with excellent catalytic activity for 4-nitrophenol reduction. Materials Science and Engineering C, 2017, 78, 429-434.	7.3	30
54	Phage capsid protein-directed MnO <sub>2</sub> nanosheets with peroxidase-like activity for spectrometric biosensing and evaluation of antioxidant behaviour. Chemical Communications, 2017, 53, 5216-5219.	4.1	94

#	Article	IF	CITATIONS
55	Novel biotemplated MnO2 1D nanozyme with controllable peroxidase-like activity and unique catalytic mechanism and its application for glucose sensing. Sensors and Actuators B: Chemical, 2017, 252, 919-926.	7.8	107
56	Facile synthesis of multicolor photoluminescent polymer carbon dots with surface-state energy gap-controlled emission. Journal of Materials Chemistry C, 2017, 5, 10785-10793.	5.5	115
57	Gold nanoprobe functionalized with specific fusion protein selection from phage display and its application in rapid, selective and sensitive colorimetric biosensing of Staphylococcus aureus. Biosensors and Bioelectronics, 2016, 82, 195-203.	10.1	93
58	Genetically Engineered Phage-Templated MnO <sub>2</sub> Nanowires: Synthesis and Their Application in Electrochemical Glucose Biosensor Operated at Neutral pH Condition. ACS Applied Materials & Interfaces, 2016, 8, 13768-13776.	8.0	106
59	A sensitive acetylcholinesterase biosensor based on gold nanorods modified electrode for detection of organophosphate pesticide. Talanta, 2016, 156-157, 34-41.	5.5	100
60	A sialic acid aldolase from Peptoclostridium difficile NAPO8 with 4-hydroxy-2-oxo-pentanoate aldolase activity. Enzyme and Microbial Technology, 2016, 92, 99-106.	3.2	6
61	A Label-Free Electrochemical Impedance Cytosensor Based on Specific Peptide-Fused Phage Selected from Landscape Phage Library. Scientific Reports, 2016, 6, 22199.	3.3	70
62	Rational design of xylose dehydrogenase for improved thermostability and its application in development of efficient enzymatic biofuel cell. Enzyme and Microbial Technology, 2016, 84, 78-85.	3.2	26
63	A Novel Scheme to Obtain Y <sub>2</sub> O <sub>2</sub> S:Er <sup>3+</sup> Upconversion Luminescent Hollow Nanofibers via Precursor Templating. Journal of the American Ceramic Society, 2015, 98, 2817-2822.	3.8	10
64	A V2O3-ordered mesoporous carbon composite with novel peroxidase-like activity towards the glucose colorimetric assay. Nanoscale, 2015, 7, 11678-11685.	5.6	100
65	Novel glucose sensor with Au@Ag heterogeneous nanorods based on electrocatalytic reduction of hydrogen peroxide at negative potential. Journal of Electroanalytical Chemistry, 2015, 742, 84-89.	3.8	18
66	Au@Ag Heterogeneous Nanorods as Nanozyme Interfaces with Peroxidase-Like Activity and Their Application for One-Pot Analysis of Glucose at Nearly Neutral pH. ACS Applied Materials & Interfaces, 2015, 7, 14463-14470.	8.0	237
67	Leaf-templated synthesis of 3D hierarchical porous cobalt oxide nanostructure as direct electrochemical biosensing interface with enhanced electrocatalysis. Biosensors and Bioelectronics, 2015, 63, 145-152.	10.1	154
68	Ultrasensitive electrochemical sensor for p-nitrophenyl organophosphates based on ordered mesoporous carbons at low potential without deoxygenization. Analytica Chimica Acta, 2014, 822, 23-29.	5.4	41
69	Porous gold cluster film prepared from Au@BSA microspheres for electrochemical nonenzymatic glucose sensor. Electrochimica Acta, 2014, 138, 109-114.	5.2	82